High Order Voltage and Current Harmonic Mitigation Using the Modular Multilevel Converter STATCOM

Kontos, Epameinondas; Tsolaridis, Georgios; Teodorescu, Remus; Bauer, Pavol

DOI
10.1109/ACCESS.2017.2749119

Publication date
2017

Document Version
Final published version

Published in
IEEE Access

IEEE Access
Multidisciplinary | Rapid Review | Open Access Journal

SPECIAL SECTION ON POWER QUALITY AND HARMONICS ISSUES OF FUTURE AND SMART GRIDS

Received July 28, 2017, accepted August 30, 2017, date of publication September 4, 2017, date of current version September 19, 2017.

Digital Object Identifier 10.1109/ACCESS.2017.2749119

High Order Voltage and Current Harmonic Mitigation Using the Modular Multilevel Converter STATCOM

EPAMEINONDAS KONTOS[1], (Member, IEEE), GEORGIOS TSOLARIDIS[2], REMUS TEODORESCU[2], (Fellow, IEEE), AND PAVOL BAUER[1], (Senior Member, IEEE)

[1]Delft University of Technology, 2628 CD Delft, The Netherlands
[2]Aalborg University, 9100 Aalborg, Denmark

Corresponding author: Epameinondas Kontos (e.kontos@tudelft.nl)

ABSTRACT Due to the increase of power electronic-based loads, the maintenance of high power quality poses a challenge in modern power systems. To limit the total harmonic distortion in the line voltage and currents at the point of the common coupling (PCC), active power filters are commonly employed. This paper investigates the use of the multilevel modular converter (MMC) for harmonics mitigation due to its high bandwidth compared with conventional converters. A selective harmonics detection method and a harmonics controller are implemented, while the output current controller of the MMC is tuned to selectively inject the necessary harmonic currents. Unlike previous studies, focus is laid on the experimental verification of the active filtering capability of the MMC. For this reason an MMC-based double-star STATCOM is developed and tested for two representative case studies, i.e., for grid currents and PCC voltage harmonics. The results verify the capability of the MMC to mitigate harmonics up to the thirteenth order, while maintaining a low effective switching frequency and thus, low switching losses.

INDEX TERMS Active power filters, harmonics, MMC, STATCOM.

I. INTRODUCTION

A major problem in modern power systems is the reduction of power quality due to the introduction of harmonic content by various power electronic-based loads. The current harmonics can cause voltage fluctuations and malfunction of electronic equipment. One of the biggest challenges of the grid operators is to keep the power quality standards high, by limiting the line voltage and currents' Total Harmonic Distortion (THD) at the Point of Common Coupling (PCC) [1].

The techniques for harmonic elimination can be divided into three main categories, i.e. passive, active and hybrid filtering [2]. The use of Passive Power Filters (PPF) is well-established, especially for low voltage systems. In this case, inductors and capacitors are tuned to mitigate specific harmonic content thereby, improving power quality. However, in medium/high voltage systems, the size and cost of PFFs increases, while several unwanted side effects appear, such as ringing transient response and resonance [3], [4]. Moreover, PPFs have limitations such as difficulty in tuning, fixed filter frequency and resonance due to matching with line impedance [5]. As a result, active filtering topologies are investigated [4].

Active and hybrid filters are commonly used in industrial applications. An Active Power Filter (APF) is a power electronic converter designed to a fraction of the load power, which is used for harmonic filtering and is connected close to the non-linear load or at the PCC [6]. With the recent improvements in the ratings and the switching behavior of power semiconductor devices, APFs are increasingly used to overcome the PPF drawbacks [5]. APFs are able to detect the load current harmonics and generate a compensating current using an output current controller [6].

Voltage-Source Converters (VSCs) are commonly used for harmonic mitigation [7]. Moreover, conventional multilevel converter topologies such as Flying Capacitor Converter (FCC), three-level diode Neutral Point Clamped (NPC) converter and Cascaded H-Bridge converter (CHB) are used for power quality improvement in different applications. In the last decade, Modular Multilevel Converter (MMC) has been introduced for high voltage (HVDC), as well as for medium voltage (STATCOM) applications. Apart from the advantages over the conventional topologies due to its modularity and scalability, the inclusion of many submodules results in a low effective switching frequency of the

submodule power semiconductor devices, while maintaining a high switching frequency of the converter, and therefore, in an increased effective control bandwidth without compromising the converter's efficiency. Using the available bandwidth in the MMC, it is possible to increase the accuracy of harmonic elimination in lower order harmonics, while at the same time being able to control higher order harmonics [8]. The aforementioned advantages make the MMC promising for APF applications [9].

Different control strategies can be used for the current and voltage harmonics compensation to improve the THD. These control strategies are based on detection of harmonics through measurement of either the load and converter currents or the grid voltage and current. Several open-loop control schemes using grid voltage feed-forward have been proposed to compensate the grid harmonic voltage [10]–[13], but they are not sufficient to suppress line current harmonics due to dead time effect [14]. Feed-forward compensation for line current harmonics can also be implemented by first extracting the current harmonic components using high pass filters in the stationary reference frame. At medium voltage and low current, there is little margin for error and thus, feed-forward compensation schemes are not preferred, whereas feedback-based approaches are recommended [14].

When proportional-resonant (PR) controllers or PI-resonant controllers are used for harmonic compensation, two possible implementations arise. The first is to use a single frame for each n^{th} harmonic rotating at frequency $n\omega$. The second is to use nested frames. More specifically, two controllers in two frames rotating at $(n+1)\omega$ and $-(n+1)\omega$ can be implemented in the main synchronous frame [10]. Both implementations are equivalent in terms of computational burden [10] and thus, high bandwidth is necessary for the current control loops in order to have satisfactory results in the elimination of steady-state errors [14]. Additionally, predictive harmonic control has been proposed and validated in [15]. However, the controller design is demanding in terms of tuning and depends on the application. Moreover, a non-optimized design can increase the computational burden and the hardware utilization significantly.

An investigation of the performance of the MMC in the mitigation of harmonics can be found in [16] and [17]. These studies consider a hybrid structure of the MMC with 'fundamental' cells, which are intended to compensate the fundamental input power factor and the 'harmonic' cells, whose number depends on the number of harmonics that need to be compensated. A PI controller and a static decoupler are used to determine the modulation of each cell, which is used to cancel a specific load current harmonic. However, in this case the MMC design becomes more complex without a significant benefit in efficiency, while redundant submodules switching at high frequencies are used, which could unnecessarily increase the cost and volume of the system. More studies have also investigated the use of MMC as APF [8], [9], [18]. However, these studies consider only average simulation models without experimental validation, which in this case is essential, since simulation studies neglect the non-linearities and delays introduced in the real system, as well as quantization errors due to the ADC interface and accuracy limitations of the sensors.

Recent grid codes require the mitigation of high order harmonics of current and voltage, which cannot be easily accomplished with conventional converters [19], [20]. This paper proves that even a 5-level MMC-based APF is able to mitigate such high harmonics without increasing its switching frequency and thus, its losses. Contrary to existing literature on MMC applications as APF, this is achieved through extensive experimental results, which are obtained using a developed MMC prototype in a laboratory set-up for two representative case studies, i.e. for current and voltage harmonics mitigation. More specifically, in this study the performance of the MMC STATCOM topology is evaluated in the mitigation of voltage and current harmonics at the PCC up to the 13^{th} order and the results on the THD and individual harmonic components are compared to limits as specified by National Grid data [21]. To achieve this, a simple harmonics detection method is applied using Low-Pass Filters (LFP) in dq-frame. The voltage and current harmonics are controlled first using PI controllers, which generate the reference for the output current harmonic components and subsequently, PR controllers are used in parallel to the fundamental output current control loop of the MMC.

The paper is structured as follows: Section II introduces the control strategy used for the current and voltage harmonics detection and elimination and the tuning of the required filters and controllers is thoroughly explained. In Section III the laboratory set-up of the MMC STATCOM is presented. The case study and the obtained results for the current harmonics are presented in Section IV, while Section V presents experimental results for the voltage harmonics elimination. Section VI summarizes the main conclusions drawn from the analysis.

II. HARMONIC MITIGATION CONTROL SCHEME

In this study an MMC-based STATCOM is used in Double-Star (DS) configuration with half-bridge submodules, as shown in Fig. 1. This configuration has been extensively studied [22], [23] and has been shown to be superior against the topology with delta-connected Full-Bridge (FB) submodules (FB-D), especially regarding negative sequence current injection [24].

The control overview of the MMC DS-STATCOM is presented in Fig. 2. More specifically, the energy controllers and the circulating current controller follow the structure presented in [25] and are tuned accordingly to provide the circulating voltage reference $v^*_{c,j}$, where j denotes the phase. The V_{dc} and Q outer controllers are implemented as PI in the dq-frame and control the d- and q-components of the current i respectively. This control structure is common in VSC converters and is presented in [27, Fig. 12.7]. The reference of the i_{dq} is then transformed into $\alpha\beta$-reference frame, i.e. $i^*_{\alpha\beta}$. An additional control loop is introduced for the

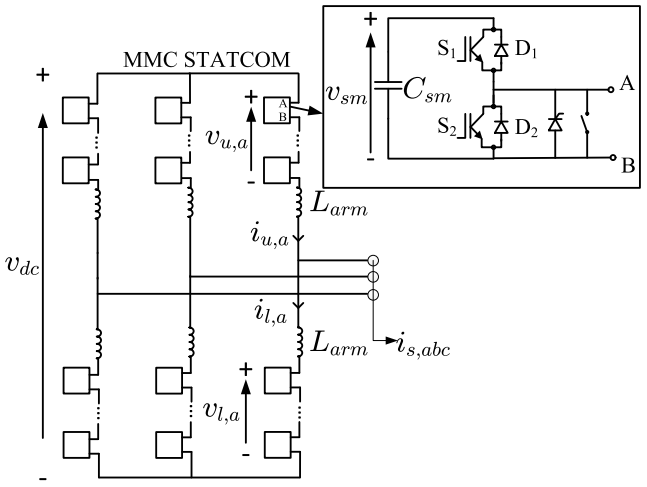

FIGURE 1. MMC DS-STATCOM schematic.

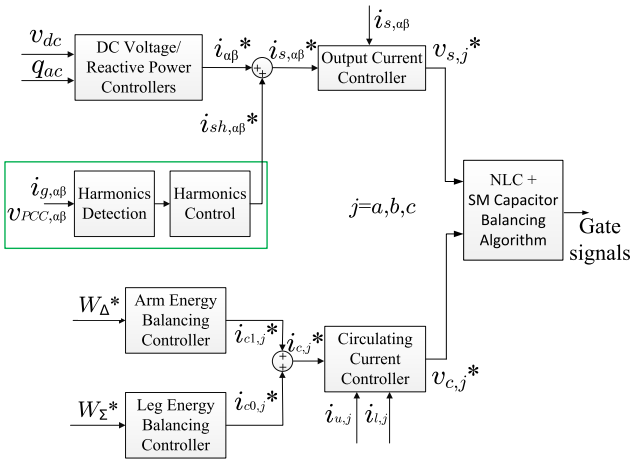

FIGURE 2. MMC control structure including harmonics.

harmonics mitigation including two steps, namely (i) detection and (ii) harmonics control. This loop provides the reference for the harmonic components of the output current $i^*_{sh,\alpha\beta}$, which is added to the outer controllers reference $i^*_{\alpha\beta}$ and is subsequently fed to the output current controller. The generated output voltage reference $v^*_{s,j}$ and the $v^*_{c,j}$ are then used to determine the number of submodules to be inserted in each arm. In this study, the submodule gate signals are determined using Nearest Level Control (NLC) and a simple submodule capacitor balancing algorithm as presented in [27]. This Section focusses on the harmonics control loop and the output current controller.

A. HARMONICS DETECTION

The measured grid current or the PCC voltage is fed to the harmonic detection block, as shown in Fig. 2. Regarding the detection methods, various techniques have been investigated in literature [28]–[30]. The methods are usually divided into two main categories: i) the selective detection methods that detect the magnitude of each harmonic individually and ii) the non-selective methods that simply split the current into fundamental and non-fundamental components [29].

In this study, a selective detection method is implemented in the dq-reference frame and the positive and negative-sequence components are both extracted for each harmonic with the appropriate rotation. The detection method as well as the reference frame transformation are usually associated with time delays arising from sampling frequency [31]. Because the filters are non-ideal and can introduce a phase shift, the reference signal might be different in shape or phase than the harmonic which needs to be attenuated [32]. Moreover, the trade-off between the filter's response and its attenuation is well-known [33]. These effects on the detection method are discussed in [7], where a comparison of different detection methods is conducted and the limitations of the active filtering procedure are highlighted. Additionally, in this case, the angular position is necessary and needs to be obtained from the PLL. This requires careful implementation especially in cases of unbalances. Therefore, these effects need to be taken into consideration in the real system and thus, transformation to both positive and negative-sequence reference frame is required to compensate for possible errors [34], [35].

Previous studies have shown that mapping the harmonic components to dc signals is more effective in detection and easier in implementation than the use of bandpass filters tuned for each harmonic in $\alpha\beta$- or abc-frame [36]. Therefore, a second-order low-pass filter (LPF) is used to extract the dc component that corresponds to the desired frequency component in the abc-reference frame. A Butterworth second-order LPF is implemented using Second-Order Generalized Integrator (SOGI) [37], and its transfer function is given by:

$$G(s) = \frac{k_{SOGI}\omega'^2}{s^2 + k_{SOGI}\omega' s + \omega'^2} \tag{1}$$

where k_{SOGI} is the gain of the LPF and ω' is the cutoff frequency in rad/s. In this case study, the parameters are selected as: k_{SOGI}=$\sqrt{2}$ and ω'=100 rad/s.

The grid current harmonics detection takes place as shown in Fig. 3.

B. HARMONICS CONTROL

The output of the LPF is compared to zero, which is the desired harmonic content. To compensate for static errors in the harmonics detection, the formulated error is then passed through a PI controller to create the harmonic reference for the output current controller. The aim of this study is to compensate harmonics up to the 13^{th} order, namely 5^{th}, 7^{th}, 11^{th} and 13^{th} which have the highest amplitude. As a result, the harmonic reference generation block includes eight PI controllers in parallel (positive and negative sequence for each harmonic order). Since every PI controller has infinite gain at 0 Hz, the desired frequencies of 250 Hz, 350 Hz, 550 Hz and 650 Hz are achieved by the rotation of the sensed current in the dq-frame.

It should be noted that the focus of these controllers is laid on the steady state performance and stability. As a result, a small integral part is used to reduce the steady-state error

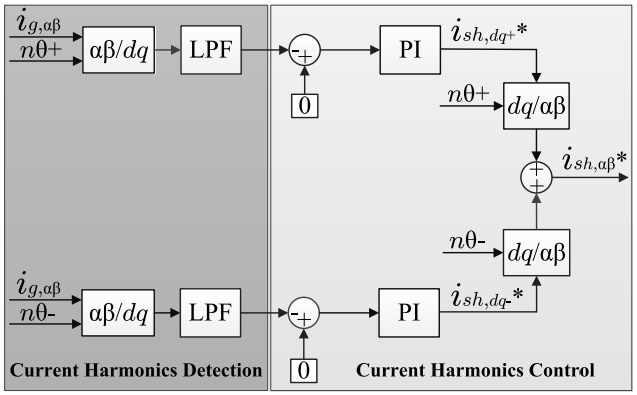

FIGURE 3. Detection and control structure for the mitigation of high order current harmonics. The grid currents are sensed and transformed with appropriate *dq*-transformations both in the positive and the negative sequence. The PI controller eliminates the resulting dc static error. The currents are transformed back to the $\alpha\beta$-frame since the output current controller (see Fig. 4) uses parallel PR controllers as described in [38].

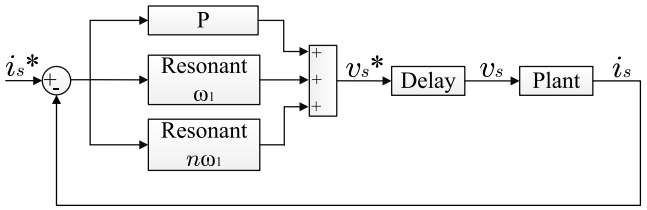

FIGURE 4. Output current controller including resonant controllers for n^{th} harmonic order.

provided that the output current controller can follow the harmonic currents reference fast and precisely. The current harmonics control structure is shown in Fig. 3.

The resulting harmonic current reference i^*_{sh} is added to the outer controller reference and fed to the output current controller as can be seen in Fig. 4. Since the output current reference i^*_s includes more harmonics than the fundamental and the control is implemented in the $\alpha\beta$-frame using PR control, four resonant controllers are added in parallel, tuned at the aforementioned desired frequencies.

The harmonic resonant controllers need to be tuned faster than the fundamental one. Therefore, depending on the higher frequency component they need to follow, the resonant parts of the output current controller are chosen as:

$$K_{R_n} = nK_{R_1} \tag{2}$$

where K_{R_1} is the fundamental resonant gain, K_{R_n} is the resonant gain of the n^{th} harmonic and n is the order of the harmonic component.

The reference output voltage v^*_s is fed to the modulation, which inserts a time delay in the loop before creating the v_s. The output voltage drives an output current through an impedance with a primarily inductive part $L_{arm}/2$. Therefore, the plant function is given by:

$$\frac{i_s}{v_s} = \frac{2}{sL_{arm}} \tag{3}$$

The ability of the MMC-STATCOM output current control to follow higher order harmonics was experimentally tested.

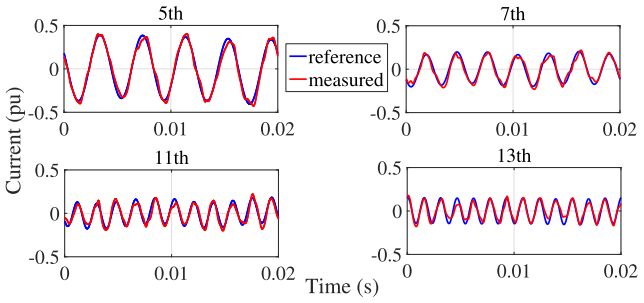

FIGURE 5. Performance of the current controller of the MMC DS-STATCOM in following sinusoidal reference currents up to the 13^{th} order.

Fig. 5 shows the measured value of the harmonic current compared to the reference. It should be noted that in all cases, the magnitude of the injected current shown is the maximum that could be controlled without saturating the voltage reference. From the results, it can be deduced that the developed controller follows with high accuracy the 5^{th} and 7^{th} harmonic order reference. The accuracy is slightly deteriorated in the 11^{th} and 13^{th} harmonic order due to the higher dynamic of the current reference that needs to be followed. However, the result can be considered adequately accurate.

C. VOLTAGE HARMONICS CONTROL

To achieve voltage harmonic components mitigation, the same detection method is used to extract the dc component of the PCC voltage harmonics. The main difference lies on the voltage harmonics control. Firstly, the references for the voltage harmonic components $v^*_{PCC,n}$, as specified by grid codes and TSOs [21], are used. Secondly, a transformation of the voltage reference output of the PI controller to current is necessary before it is fed to the output current controller. For this purpose, the line impedance Z_{nh} value needs to be estimated for each n^{th} harmonic order and is used as shown in Fig. 6.

III. EXPERIMENTAL SET-UP

To test the active filtering capability of the MMC DS-STATCOM, a laboratory set-up was built. The MMC STATCOM prototype is shown in Fig. 7, while Table 1 summarizes the main parameters of the lab-scaled system.

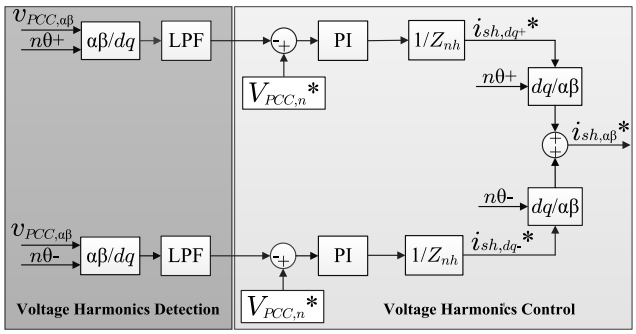

FIGURE 6. Voltage harmonics detection and control.

FIGURE 7. Laboratory prototype of MMC DS-STATCOM.

TABLE 1. Parameters of experimental setup.

Description	Symbol	Value
Rated Power (kVA)	S	1.25
Rated Phase RMS Voltage (V)	V_g	150
Pole-to-pole Voltage (V)	V_{dc}	400
Submodule's Capacitance (mF)	C_{sm}	4
Arm Inductance (mH)	L_{arm}	20
Number of Submodules per arm	N	4
Transformer Ratio	n	$1{:}\sqrt{3}$

TABLE 2. Controller gains of lab setup in rad/s.

Controller	K_p	K_i	K_r
Arm Energy	0.2	0.5	-
Leg Energy	0.2	0.3	-
Circulating Current	20	800	ω_1: 8×10^3 ω_2: 8×10^3
Output Current	24	-	ω_1: 2.4×10^3; ω_5: 12×10^3; ω_7: 16.8×10^3; ω_{11}: 26.4×10^3; ω_{13}: 31.2×10^3
DC Voltage	0.15	1	-
Reactive Power	0.15	1	-
Harmonics	1	0.01	-

The MMC is controlled via an FPGA that is part of the dSPACE simulator, which acts as the central controller and is connected to a PC equipped with ControlDesk interface. The control algorithm of the MMC was implemented in Matlab/Simulink and HDL code was automatically generated and loaded to the FPGA of the dSPACE interface. The communication of the dSPACE simulator to the submodules of the MMC takes place via optical transmission (i.e. optical fibers) to provide the necessary isolation and noise immunity. The submodules send the capacitor voltage measurement and a fault indication signal to the dSPACE, while dSPACE sends the necessary PWM signals to the submodule switches. The sampling frequency was 10 kHz and the gains for the different employed controllers are presented in Table 2. Details on the set-up connection for the investigated current and voltage harmonics mitigation case studies are given in Sections IV and V respectively.

IV. EXPERIMENTAL RESULTS ON CURRENT HARMONICS MITIGATION

In this Section, the ability of the MMC to act as an active filter and attenuate the current harmonics is evaluated experimentally. A diode rectifier load is connected to the PCC as shown in the schematic of Fig. 8.

An ideal AC source is used to simulate the grid. This is connected to a Dy11n isolation transformer and a diode bridge rectifier is placed in parallel to the STATCOM.

On the DC side of the bridge rectifier, a resistor R of 200 Ω is connected. This load is highly non-linear and draws a harmonic current [39]. This current is being drawn from the ac grid resulting in polluted grid current waveforms which may have a severe impact on sensitive loads connected to the PCC. The grid currents are sensed and fed to the control system, as described in Section II. The aim is the elimination of the current harmonics up to the 13^{th} order, using a relatively low effective switching frequency (≈1 kHz), which is mainly determined by a simple sorting algorithm that is employed to ensure the balanced operation of the submodules within one arm [27].

Fig. 9 depicts the currents when STATCOM operates close to its nominal power, injecting 0.73 pu of inductive reactive current to the grid and the harmonic compensation is not activated. The total current flowing to the grid is highly

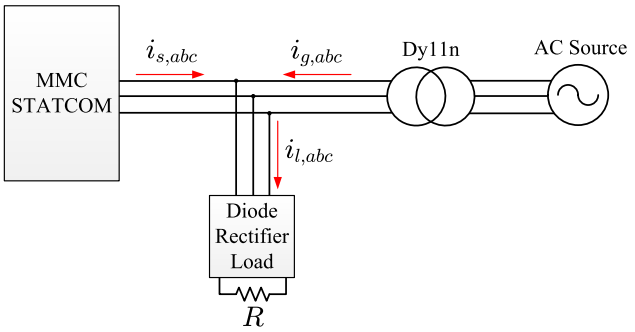

FIGURE 8. Schematic of experimental set-up for current harmonic mitigation.

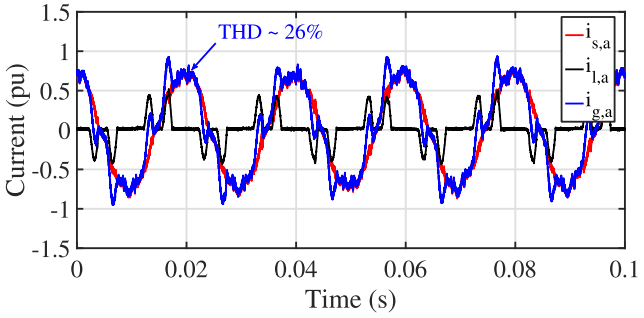

FIGURE 9. DS-STATCOM current (red), load current (black) and grid current (blue) at the PCC of phase-a without harmonic compensation. Grid current has a %THD of 26%.

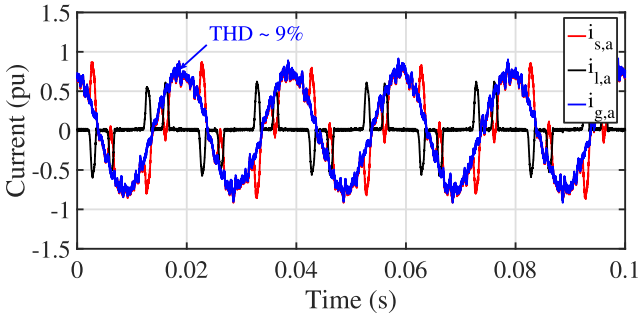

FIGURE 10. DS-STATCOM current (red), load current (black) and grid current (blue) at the PCC of phase-a with harmonic compensation. Grid current has now a %THD of 9%.

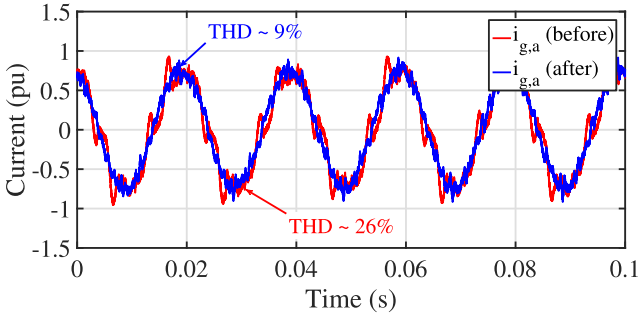

FIGURE 11. Grid current at the PCC of phase-a before (red) and after (blue) harmonic compensation - Time domain. The %THD is reduced by 15%.

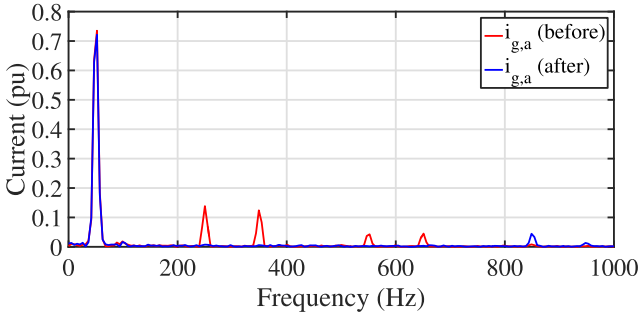

FIGURE 12. Grid current at the PCC of phase-a before (red) and after (blue) harmonic compensation - Frequency domain. The target harmonics are completely eliminated.

distorted with approximately 26% THD, mainly due to the presence of the 5^{th}, 7^{th}, 11^{th} and 13^{th} order current harmonics.

Fig. 10 depicts the current waveforms after the application of the harmonic compensation. It can be seen that the STATCOM currents are now distorted, while the THD of the grid currents is effectively reduced to 9%.

A comparative graph in Fig. 11 shows the grid currents before and after the application of the harmonic compensation in the time domain, while Fig. 12 depicts the result of the Fast Fourier Transformation (FFT) of the grid current waveforms. It can be seen that the injection strategy eliminates almost completely the targeted harmonic components in the grid current, which now appear in the STATCOM output current. The resulting distortion for each individual harmonic order is well within the limits defined in [19].

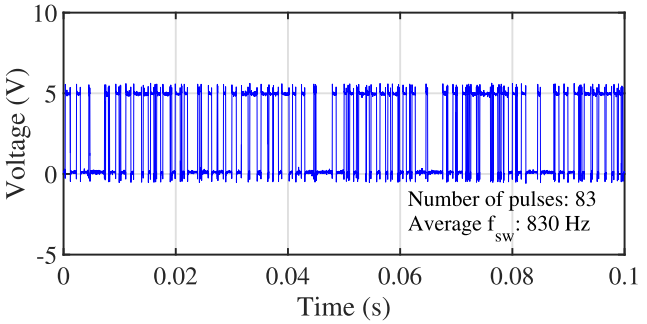

FIGURE 13. PWM signals of first submodule of phase-a when the harmonic compensation is enabled. The sorting algorithm ensures approximately equal switching frequency for all submodules.

To estimate the average switching frequency of one submodule when the harmonic compensation was activated, the PWM signal voltage pulses were monitored for several cycles. Fig. 13 shows only the recorded number of PWM pulses fed to the first submodule of phase-a in 100 ms. However, it can be considered that on average the switching frequency is similar for all submodules. It can be seen that the average effective switching frequency is approximately 0.83 kHz, which is well within the limit of 1 kHz. This result is particularly important since it proves that the MMC-STATCOM can efficiently mitigate high order of harmonics (up to 650 Hz) with the use of low switching frequency due to its increased bandwidth.

V. EXPERIMENTAL RESULTS ON VOLTAGE HARMONICS MITIGATION

Apart from current harmonics, problems can be created by the presence of voltage harmonics, which is a common phenomenon in weak grids, e.g. in wind power plants. To mitigate this problem, STATCOMs are often utilized [40]–[42]. In this Section, the ability of the developed control system to attenuate harmonics at the PCC voltages is assessed experimentally.

The schematic of the used experimental set-up is shown in Fig. 14. In this case, the controllable AC source is used to emulate the behavior of the wind power plant and is connected to the isolation transformer through a 2.2 *mH* line inductor to emulate the behavior of a grid line.

The harmonics injected by the AC source are controlled and a desired waveform is generated. The control system is then responsible to sense the harmonic content of the voltage and with the appropriate current injection it should be able to mitigate them, respecting the limits of the grid operator for

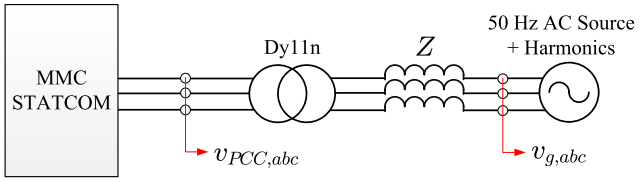

FIGURE 14. Schematic of experimental setup for voltage harmonic mitigation.

TABLE 3. Voltage Harmonics at the PCC.

Harmonic order	Grid voltage	Specified limit
2^{nd}	-	0.8 %
5^{th}	3.3 %	2 %
7^{th}	2.1 %	0.59 %
11^{th}	1.7 %	0.64 %
13^{th}	-	1.5 %
17^{th}	0.7 %	0.1 %

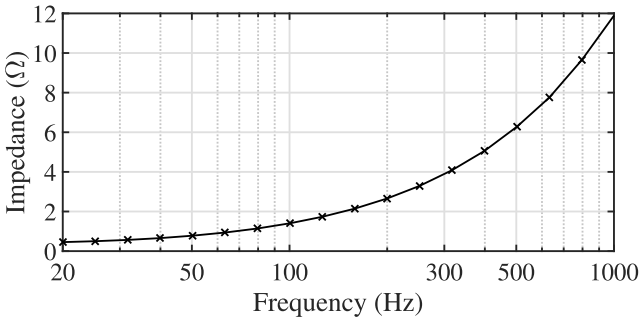

FIGURE 15. Line impedance Z measurements obtained by performing frequency sweep with an impedance analyzer.

the PCC voltage. The maximum harmonic attenuation that the STATCOM can provide is usually limited by its current rating and the limited available DC link voltage, while it also depends on the line inductance.

In this scenario the values for the injected PCC voltage harmonics and their respective limits, as set in [21], are presented in Table 3. The specified limits are used as references $V^*_{PCC,n}$ in the closed-loop control scheme presented in Fig. 6. Due to the aforementioned limitations of the converter, harmonics up to the 11^{th} order are controlled and attenuated. It should also be noted that in this case study the converter does not inject reactive current at the fundamental frequency.

A frequency sweep is conducted for the line impedance Z using an impedance analyzer and its value is measured for frequencies up to 1 kHz in order to take the effect of the parasitic elements into consideration. The respective impedance value at each frequency (Z_{nh}) is used for the control of the voltage harmonics as explained in Section II. The measurements are presented in Fig. 15.

Fig. 16 shows the comparison between the voltage at the PCC before and after the activation of the control system for harmonic mitigation. Before, the voltage at the PCC is equal to the voltage generated by the non-ideal controllable AC source taking into account the transformer ratio, since no current is flowing in the system, and the THD is 4.9%. The activation of the harmonic compensation results in a significant reduction in the THD from 4.9% to 3%, as depicted in Fig. 16, in the time domain.

Fig. 17 shows the effectiveness of the voltage mitigation control system of the MMC STATCOM with a comparative graph in the frequency domain. Considering the defined references, it can be concluded that the selectivity of the detection

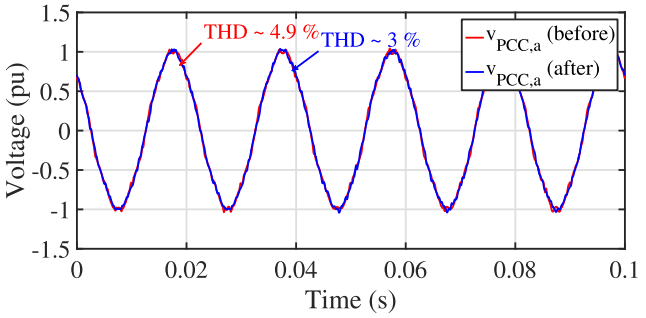

FIGURE 16. Voltage at the PCC of phase-a before (red) and after (blue) harmonic compensation - Time domain. The %THD is reduced by 1.9%.

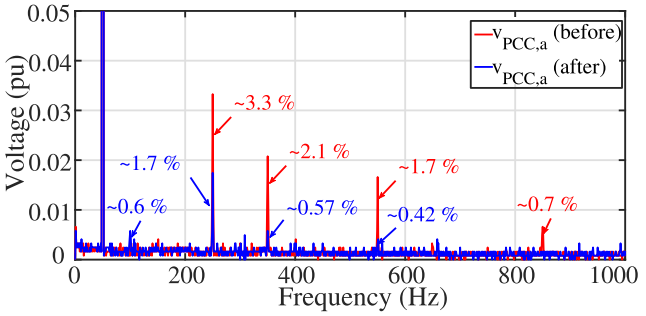

FIGURE 17. Voltage at the PCC of phase-a before (red) and after (blue) harmonic compensation - Frequency domain. The target harmonics are overcompensated.

and control method for each harmonic component is verified. Moreover, it can be seen that the harmonic components of all the frequencies of interest follow the specified values as set by the grid codes. Although closed-loop control is used, the obtained values for the harmonic components are slightly below the specified limits due to overcompensation resulting from the measurement of the line impedance Z. More specifically, the impedance values, which are used in the harmonics control (see Fig. 6), were estimated using the impedance analyzer at low currents. When the system is operated at high currents, close to saturation, the inductor impedance value can be higher than the measured one resulting in harmonics overcompensation. It has to be noted that the average effective switching frequency of the submodules in this case was once again recorded to be approximately 0.9 kHz.

VI. CONCLUSIONS

Recent grid codes require the compensation of high order current and voltage harmonics. For this reason, this study focussed on the use of the MMC as an active filter to mitigate those harmonics. A selective harmonics detection method and an output harmonic current controller were implemented and experimentally verified using a developed MMC prototype, which was operated as DS-STATCOM. Tuning was performed taking into account the non-linearities of the system and the delays introduced by the measurements and the control loop, which are usually neglected when approaching this problem through average model simulations. Finally, two realistic representative case studies for current and voltage harmonics were defined and tested.

The MMC ability to selectively inject harmonic currents up to 13^{th} order was proven, while the main limitations were set by the set-up rating, the number of levels of the MMC and the available DC link voltage. In fact, it was seen that the increased bandwidth of the MMC allowed for the grid current harmonics control up to the 13^{th} order and for PCC voltage harmonics up to the 11^{th} order, while maintaining the average effective switching frequency below 1 kHz and thus, the MMC losses low. More specifically, harmonics mitigation resulted in a reduction of the current THD from 26% down to 9% and of the voltage THD from 4.9% to 3%. Therefore, the advantages of the MMC technology were hereby proven for active filtering purposes.

REFERENCES

[1] S. M. Halpin, "Comparison of IEEE and IEC harmonic standards," in *Proc. IEEE Power Eng. Soc. Gen. Meet.*, vol. 3. Jun. 2005, pp. 2214–2216.

[2] H. A. Kazem, "Harmonic mitigation techniques applied to power distribution networks," *Adv. Power Electron.*, vol. 2013, Jan. 2013, Art. no. 591680. 591680

[3] R. N. Beres, X. Wang, M. Liserre, F. Blaabjerg, and C. L. Bak, "A review of passive power filters for three-phase grid-connected voltage-source converters," *IEEE J. Emerg. Sel. Topics Power Electron.*, vol. 4, no. 1, pp. 54–69, Mar. 2016.

[4] R. S. Rani, C. S. Rao, and M. V. Kumar, "Analysis of active power filter for harmonic mitigation in distribution system," in *Proc. Int. Conf. Electr., Electron., Optim. Techn. (ICEEOT)*, Mar. 2016, pp. 1338–1446.

[5] D. Schwanz, M. Bollen, A. Larsson, and L. H. Kocewiak, "Harmonic mitigation in wind power plants: Active filter solutions," in *Proc. 17th Int. Conf. Harmon. Quality Power (ICHQP)*, Oct. 2016, pp. 220–225.

[6] C. Lascu, L. Asiminoaei, I. Boldea, and F. Blaabjerg, "Frequency response analysis of current controllers for selective harmonic compensation in active power filters," *IEEE Trans. Ind. Electron.*, vol. 56, no. 2, pp. 337–347, Feb. 2009.

[7] R. E. Betz, T. J. Summers, and G. Mirzaeva, "Active filtering and VAR control of a cascaded H-bridge multi-level StatCom," in *Proc. Int. Conf. Power Electron. Drive Syst. (PEDS)*, Nov. 2009, pp. 816–821.

[8] J. Wu, X. Xu, Y. Liu, and D. Xu, "Compound control strategy of active power filter based on modular multilevel converter," in *Proc. 11th World Congr. Intell. Control Autom. (WCICA)*, Jun. 2014, pp. 4771–4777.

[9] M. S. Hamad, K. H. Ahmed, and A. I. Madi, "Current harmonics mitigation using a modular multilevel converter-based shunt active power filter," in *Proc. IEEE Int. Conf. Renew. Energy Res. Appl. (ICRERA)*, Nov. 2016, pp. 755–759.

[10] M. Liserre, R. Teodorescu, and F. Blaabjerg, "Multiple harmonics control for three-phase grid converter systems with the use of PI-RES current controller in a rotating frame," *IEEE Trans. Power Electron.*, vol. 21, no. 3, pp. 836–841, May 2006.

[11] M. Castilla, J. Miret, A. Camacho, J. Matas, and L. G. de Vicuna, "Reduction of current harmonic distortion in three-phase grid-connected photovoltaic inverters via resonant current control," *IEEE Trans. Ind. Electron.*, vol. 60, no. 4, pp. 1464–1472, Apr. 2013.

[12] J. Xu, Q. Qian, S. Xie, and B. Zhang, "Grid-voltage feedforward based control for grid-connected LCL-filtered inverter with high robustness and low grid current distortion in weak grid," in *Proc. IEEE Appl. Power Electron. Conf. Expo. (APEC)*, Mar. 2016, pp. 1919–1925.

[13] D. Wu and L. Peng, "Analysis and suppressing method for the output voltage harmonics of modular multilevel converter," *IEEE Trans. Power Electron.*, vol. 31, no. 7, pp. 4755–4765, Jul. 2016.

[14] S. Madhusoodhanan *et al.*, "Harmonic analysis and controller design of 15 kV SiC IGBT-based medium-voltage grid-connected three-phase three-level NPC converter," *IEEE Trans. Power Electron.*, vol. 32, no. 5, pp. 3355–3369, May 2017.

[15] Z. Shu, M. Liu, L. Zhao, S. Song, Q. Zhou, and X. He, "Predictive harmonic control and its optimal digital implementation for MMC-based active power filter," *IEEE Trans. Ind. Electron.*, vol. 63, no. 8, pp. 5244–5254, Aug. 2016.

[16] J. A. Munoz, J. R. Espinoza, C. R. Baier, L. A. Moran, J. I. Guzman, and V. M. Cardenas, "Decoupled and modular harmonic compensation for multilevel STATCOMs," *IEEE Trans. Ind. Electron.*, vol. 61, no. 6, pp. 2743–2753, Jun. 2014.

[17] J. A. Munoz, J. R. Espinoza, C. R. Baier, L. A. Moran, and J. I. Guzman, "Modular harmonic cancellation in a multilevel STATCOM," in *Proc. 37th Annu. Conf. IEEE Ind. Electron. Soc. (IECON)*, Nov. 2011, pp. 4146–4151.

[18] F. T. Ghetti, A. A. Ferreira, H. A. C. Braga, and P. G. Barbosa, "A study of shunt active power filter based on modular multilevel converter (MMC)," in *Proc. 10th IEEE/IAS Int. Conf. Ind. Appl.*, Nov. 2012, pp. 1–6.

[19] *IEEE Recommended Practice and Requirements for Harmonic Control in Electric Power Systems*, IEEE Standard 519-2014 (Revision of IEEE Standard 519-1992), Jun. 2014, pp. 1–29.

[20] *Planning Levels for Harmonic Voltage Distortion and Connection of Non-Linear Equipment to Transmission and Distribution Networks in the UK*, document Engineering Recommendation (ER) G5/4-1, Issue 4, Amendment 1, Oct. 2005.

[21] N. Grid, "Generator self build enduring regime harmonic assessment process flow," Nat. Grid, U.K., Tech. Rep., Oct. 2005.

[22] H. P. Mohammadi and M. T. Bina, "A transformerless medium-voltage STATCOM topology based on extended modular multilevel converters," *IEEE Trans. Power Electron.*, vol. 26, no. 5, pp. 1534–1545, May 2011.

[23] A. António-Ferreira, O. Gomis-Bellmunt, and M. Teixidó, "HVDC-based modular multilevel converter in the statcom operation mode," in *Proc. 18th Eur. Conf. Power Electron. Appl. (EPE'ECCE Eur.)*, Sep. 2016, pp. 1–10.

[24] G. P. Tsolaridis, H. A. Pereira, A. F. Cupertino, R. Teodorescu, and M. Bongiorno, "Losses and cost comparison of DS-HB and SD-FB MMC based large utility grade STATCOM," in *Proc. IEEE 16th Int. Conf. Environ. Electr. Eng. (EEEIC)*, Jun. 2016, pp. 1–6.

[25] G. P. Tsolaridis, E. Kontos, S. K. Chaudhary, P. Bauer, and R. Teodorescu, "Internal balance during low-voltage-ride-through of the modular multilevel converter STATCOM," *Energies*, vol. 10, no. 7, p. 935, 2017.

[26] R. Teodorescu, M. Liserre, and P. Rodríguez, *Grid Converters for Photovoltaic and Wind Power Systems*. Hoboken, NJ, USA: Wiley, 2011.

[27] K. Sharifabadi, L. Harnefors, H.-P. Nee, S. Norrga, and R. Teodorescu, *Design, Control and Application of Modular Multilevel Converters for HVDC Transmission Systems*, 1st ed. Hoboken, NJ, USA: Wiley, 2016.

[28] L. Asiminoael, F. Blaabjerg, and S. Hansen, "Detection is key—Harmonic detection methods for active power filter applications," *IEEE Ind. Appl. Mag.*, vol. 13, no. 4, pp. 22–33, Jul. 2007.

[29] P. Lauttamus and H. Tuusa, "Three-level VSI based low switching frequency 10 MVA STATCOM in reactive power and harmonics compensation," in *Proc. 7th Int. Conf. Power Electron. (ICPE)*, Oct. 2007, pp. 536–541.

[30] S. Rechka, E. Ngandui, J. Xu, and P. Sicard, "Analysis of harmonic detection algorithms and their application to active power filters for harmonics compensation and resonance damping," *Can. J. Electr. Comput. Eng.*, vol. 28, no. 1, pp. 41–51, Jan. 2003.

[31] T. Nussbaumer, M. L. Heldwein, G. Gong, S. D. Round, and J. W. Kolar, "Comparison of prediction techniques to compensate time delays caused by digital control of a three-phase buck-type PWM rectifier system," *IEEE Trans. Ind. Electron.*, vol. 55, no. 2, pp. 791–799, Feb. 2008.

[32] A. Safaee, D. Yazdani, A. Bakhshai, and P. Jain, "Three-phase harmonic detection methods for grid-connected converters," in *Proc. 26th Annu. IEEE Appl. Power Electron. Conf. Expo. (APEC)*, Mar. 2011, pp. 1357–1361.

[33] B. Shenoi, *Introduction to Digital Signal Processing and Filter Design*. Hoboken, NJ, USA: Wiley, 2005.

[34] R. Teodorescu, F. Blaabjerg, M. Liserre, and P. C. Loh, "Proportional-resonant controllers and filters for grid-connected voltage-source converters," *IEE Proc.-Electr. Power Appl.*, vol. 153, no. 5, pp. 750–762, Sep. 2006.

[35] P. R. Babu, R. Agrawal, S. R. Paital, S. S. Raju, and S. Raju, "Novel methods of detection of harmonics," *Int. J. Eng. Innov. Technol. (IJEIT)*, vol. 2, no. 11, pp. 167–173, May 2013.

[36] M. Gonzalez, V. Cardenas, and F. Pazos, "DQ transformation development for single-phase systems to compensate harmonic distortion and reactive power," in *Proc. 9th IEEE Int. Power Electron. Congr. (CIEP)*, Oct. 2004, pp. 177–182.

[37] Z. Xin, Z. Qin, M. Lu, P. C. Loh, and F. Blaabjerg, "A new second-order generalized integrator based quadrature signal generator with enhanced performance," in *Proc. IEEE Energy Convers. Congr. Expo. (ECCE)*, Sep. 2016, pp. 1–7.

[38] G. Tsolaridis, E. Kontos, H. Parikh, R. M. Sanchez-Loeches, R. Teodorescu, and S. K. Chaudhary, "Control of a modular multilevel converter STATCOM under internal and external unbalances," in *Proc. 42nd Annu. Conf. IEEE Ind. Electron. Soc. (IECON)*, Oct. 2016, pp. 6494–6499.
[39] M. Sakui and H. Fujita, "An analytical method for calculating harmonic currents of a three-phase diode-bridge rectifier with DC filter," *IEEE Trans. Power Electron.*, vol. 9, no. 6, pp. 631–637, Nov. 1994.
[40] S. K. Chaudhary, C. Lascu, R. Teodorescu, and L. H. Kocewiak, "Voltage feedback based harmonic compensation for an offshore wind power plant," in *Proc. IEEE Int. Conf. Power Electron., Drives Energy Syst. (PEDES)*, Dec. 2016, pp. 1–5.
[41] S. K. Chaudhary *et al.*, "Challenges with harmonie compensation at a remote bus in offshore wind power plant," in *Proc. IEEE 16th Int. Conf. Environ. Electr. Eng. (EEEIC)*, Jun. 2016, pp. 1–6.
[42] L. H. Kocewiak *et al.*, "Power quality improvement of wind power plants by active filters embedded in statcoms," in *Proc. 15th Int. Workshop Large-Scale Integr. Wind Power Into Power Syst. As Well As Transmiss. Netw. Offshore Wind Farms*, Nov. 2016.

EPAMEINONDAS KONTOS (M'14) received the Diploma degree in electrical and computer engineering from the National Technical University of Athens, Athens, Greece, in 2010, and the M.Sc. (*cum laude*) degree in sustainable energy technology from the Delft University of Technology, Delft, The Netherlands, in 2013. During his studies, he was an Intern for three months with SMA Solar Technology AG, Kassel, Germany. Since 2013, he has been a Ph.D. Researcher on the TKI Synergies at Sea Project with the DCE&S Group of TU Delft. His interests include the design of multi-level modular converters for HVDC applications, protection system design for multi-terminal HVDC grids, and the control of power electronics.

GEORGIOS TSOLARIDIS received the degree in electrical and computer engineering with specialization in power engineering from the Aristotle University of Thessaloniki, Greece, the Diploma degree in 2014, and the master's degree in power electronics and drives from Aalborg University, Denmark, in 2016. He is currently pursuing the Ph.D. degree with the Laboratory for High Power Electronic Systems, ETH Zurich. During his studies, he was with the ABB's Corporate Research Center, Vasteras, Sweden, as an Intern for six months.

REMUS TEODORESCU (F'12) received the Dipl.Ing. degree in electrical engineering from the Polytechnical University of Bucharest, Bucharest, Romania, in 1989, and the Ph.D. degree in power electronics from the University of Galati, Romania, in 1994. In 1998, he joined the Power Electronics Section, Department of Energy Technology, Aalborg University, Aalborg, Denmark, where he is currently a Full Professor. Since 2013, he has been a Visiting Professor with Chalmers University. His research interests include the design and control of grid-connected converters for photovoltaic and wind power systems, HVDC/FACTS based on modular multilevel converters, and storage systems based on Li-ion battery technology, including modular converters and active BMS.

PAVOL BAUER (SM'07) is currently a Full Professor with the Department of Electrical Sustainable Energy, Delft University of Technology and the Head of the DC Systems, Energy Conversion and Storage Group. He has authored or co-authored over 80 journal and 300 conference papers in his field (with h-factor Google scholar 33, Web of science 21), he is an author or co-author of eight books, holds four international patents and organized several tutorials at the international conferences. He was involved in many projects for industry concerning wind and wave energy, power electronic applications for power systems, such as Smarttrafo; HVDC systems, projects for smart cities, such as PV charging of electric vehicles, PV and storage integration, contactless charging; and he participated in several Leonardo da Vinci and H2020 EU projects as a Project Partner (ELINA, INETELE, E-Pragmatic) and Coordinator (PEMCWebLab.com-Edipe, SustEner, Eranet DCMICRO). He is a Former Chairman of Benelux IEEE Joint Industry Applications Society, Power Electronics and Power Engineering Society Chapter, the Chairman of the Power Electronics and Motion Control Council, a member of the Executive Committee of European Power Electronics Association, and also a member of International Steering Committee at numerous conferences.